Inorganic Chemistry

Article

pubs.acs.org/IC

Metal Binding of Flavonoids and Their Distinct Inhibition Mechanisms Toward the Oxidation Activity of Cu^{2+}–β-Amyloid: Not Just Serving as Suicide Antioxidants!

William Maung Tay,[†] Giordano F. Z. da Silva,[‡] and Li-June Ming*

Department of Chemistry, University of South Florida, Tampa, Florida 33620-5250, United States

ABSTRACT: The accumulation of plagues of β-amyloid (Aβ) peptides in the brain is a hallmark of Alzheimer's disease (AD). The redox-active Cu and Fe complexes of Aβ can cause damage to the neurons potentially via reactive oxygen species (ROS). The significant metal-mediated oxidative activity of CuAβ suggests that its presence can be chemically devastating regardless whether it is a cause or a result of AD. Flavonoids exhibit various benefits to human health, attributable to their metal-binding and antioxidation activities to certain extents. Despite broad interests and extensive studies of their metal-binding properties and anti/pro-oxidation activities, these properties and the mechanisms of the activities toward metal-centered oxidation reactions have not been fully revealed and concluded. We report herein distinctive antioxidation mechanisms between two flavonoid families toward the oxidation reactions by $CuA\beta_{1-20}$, wherein the flavonols quercetin (Qr) and myricetin (Mr) competitively inhibit the oxidation of catechol by $CuA\beta_{1-20}$ with K_i of 11.2 and 32.6 μM, respectively, whereas the flavanols catechin (Ct) and epicatechin (Et) are substrates with k_{cat} = 1.01×10^{-2} and 1.55×10^{-3} s^{-1} and K_m = 0.94 and 0.55 mM, respectively. Qr has a nearly 10-fold higher antioxidative efficacy than Ct against the oxidation activity of CuAβ, while Ct is effectively oxidized, which further decreases its antioxidant capacity. Similar inhibition patterns are observed toward oxidation of the catecholamine neurotransmitter dopamine by $CuA\beta_{1-20}$. Metal ions and CuAβ bind Qr with a 1:1 ratio under our experimental conditions through the α-ketoenolate moiety as determined by the use of Co^{2+} and Yb^{3+} as paramagnetic NMR probes. Unlike flavanols, which are merely suicide antioxidative substrates, flavonols bind to the metal center and prevent metal-mediated redox reactions. We suggest flavonols may serve as leads for drug discovery and/or as agents toward preventing metal-mediated oxidative stress due to AD and other disorders. Moreover, CuAβ shows 8.6- and 4.2-fold higher kinetic regioselectivity in terms of k_{cat} and k_{cat}/K_m, respectively, toward the peroxidation of Ct than that of the enantiomer Et, suggesting potential development of metallo-catalysts in regioselective catalysis by the use of metallopeptides as templates.

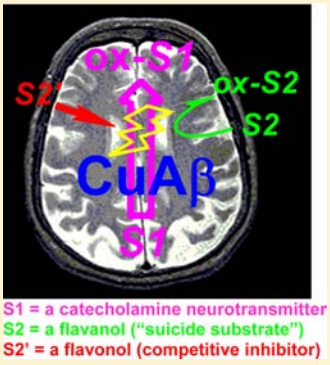

INTRODUCTION

Aggregated beta-amyloid (Aβ) peptides of 40−42 amino acids (DAEFR **H**DSGY EV**HH**Q KLVFF AEDVG SNKGA IIGLM VGGVV IA) found in plaques in the hippocampus and neocortical regions of the human brain are considered a hallmark of the neuropathology of the neurodegenerative Alzheimer's disease (AD),[1] despite continuous debates about their roles in AD.[2] Aβ is a proteolytic product of a membrane-spanning amyloid precursor protein upon sequential cleavage by β and γ secretases.[3,4] The amphipathic nature of Aβ renders its interaction with anionic and hydrophobic components of cell membranes[5,6] and induces cytotoxicity.[7] Furthermore, α- and β-secretases[8] and insulin degrading enzyme[9] can produce $A\beta_{1-16}$ and $A\beta_{1-20}$ fragments that contain three histidine residues reported to be the metal coordinating residues in Aβ.[10,11] Metal binding to Aβ can affect the structure and reactivity of this peptide.[12] Zn^{2+}, Cu^{2+}, and Fe^{3+} are found in high concentrations in Aβ plaques[13] and have been shown to induce Aβ aggregation *in vitro*.[14] The interaction of Cu^{2+} with His side chains of Aβ has been demonstrated by NMR and EPR spectroscopic methods.[10,11] Redox-active metal complexes of Aβ such as Cu^{2+} and Fe^{3+} complexes can generate reactive oxygen species (ROS) and contribute to neurotoxicity through ROS-mediated oxidative stress in AD.[1,15,16] We have recently shown that Cu^{2+} complexes of Aβ and their fragments exhibited metal-mediated oxidation/hydroxylation of catechol and phenol and their biological derivatives such as neurotransmitters,[11,17] corroborating the role of metallo-Aβ in causing oxidative stress and contributing to the neuropathology in AD.[1,8,9] Consequently, natural antioxidants that can cross the blood-brain barrier[18] and also bind metal ion(s) would be good candidates as drug leads and/or protective agents against imbalance of redox reactions and metal metabolism in AD. Flavonoids found in fruits and vegetables fit the criteria[19] that can serve as the leads for drug discovery and for further improvement of their bioavailability and function.[20]

Flavonoids are ubiquitously distributed in plants, and some display antimicrobial and antifungal properties that largely contribute toward growth and development of plants.[21] Flavonoids show various beneficial properties toward human health such as antihepatotoxic, antiinflammatory, antiathero-

Received: August 21, 2012
Published: January 9, 2013

   dx.doi.org/10.1021/ic301832p | *Inorg. Chem.* 2013, 52, 679−690

genic, antiallergenic, antiosteoporotic, antibiotic, antiviral, anticancer, and neuroprotective properties,[22] despite their potential toxicity at pharmaceutical concentrations.[23] Their structural versatility affords wide biological activities, including signaling,[24] interactions with enzymes,[25] free radical scavenging,[26] and metal binding.[27] The prototypical flavonoids (Figure 1) catechin (Ct) and quercetin (Qr) are abundant in tea, red

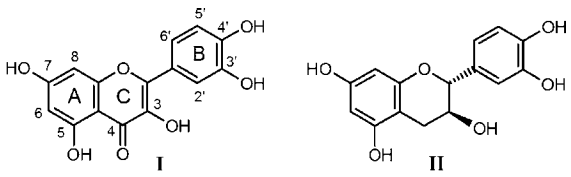

Figure 1. Structure of quercetin (Qr; **I**) of the flavonol family and (+)-catechin (Ct; **II**) of the flavanol family. Three possible metal-binding sites are available in Qr: β-ketophenolate (at positions 4 and 5), α-ketoenolate (at 3 and 4), and catechol moiety (at 3′ and 4′). The stereochemistry at 3-OH in (−)-epicatechin (Et) is opposite to that of Ct. Myricetin (Mr) is a flavonol with OH groups at position 3′, 4′, and 5′, while the flavonol morin has OH substituents at 2′ and 4′. The simple flavonoids 3- and 5-hydroxyflavone (3Hf and 5Hf) have only one OH group at positions 3 and 5, respectively.

wine, cocoa, and various fruits and vegetables, and more significantly are able to cross the blood-brain barrier.[18] They exhibit significant biological activities that may be related to their health benefits, such as antioxidation toward plasma,[28] low-density lipoprotein,[29] and DNA,[30] prevention of amyloid-induced apoptosis,[31] neuroprotective properties,[32] and increase in the lifespan of *Caenorhabditis elegans*.[33] A short-term dietary Qr treatment can increase its level in the brain of mice, yet has no effect on mRNA levels for expression of genes related to antioxidants and AD.[34] Qr can also protect the striatum in the rat model of Parkinson's disease against oxidative stress and reduce dopaminergic neuronal loss.[35] In addition to providing protection against Aβ-induced oxidative cellular toxicity,[36] flavonoids and polyphenols can also prevent Aβ fibril formation,[37] thus may serve a dual role against Cu^{2+}−Aβ toxicity.

Bifunctional ligands comprised of a metal-chelating and an Aβ-interacting moieties have been exploited for the purpose of better recognition and potential detoxification of Aβ, and for further revealing the roles of metallo-Aβ complexes in AD.[12] For example, flavonol analogues with a substituent 4′-dimethylamin "**FL3**" or 4′-2-pyridyl group "**FL4**" could chelate Cu^{2+} and Zn^{2+} and remove them from metallo−Aβ yet could not prevent metal-mediated aggregation of Aβ; [38] whereas the chelating agent clioquinol can disrupt the aggregation and/or oxidation chemistry of metallo−Aβ and reduce neurotoxicity[39] (however, its use is controversial[40]). Only **FL3** exhibits a significant free radical quenching activity, which however is less than the activity of the flavonol myricetin. In order to better understand the structure−activity relationship and the health benefits of natural and synthetic flavonoids, their physical and chemical properties must be clearly outlined. Although the metal bindings and antioxidant activities of flavonoids have been widely investigated,[26,27] the relationship between these two properties remains unclear. In this report, we present results about the very different antioxidative mechanisms of the two structurally diverse flavonol and flavanol families toward the metal-centered oxidative activity of Cu−Aβ_{1-20}, which is attributable to their different metal-binding properties determined by the use of paramagnetic metal ions as electronic and NMR spectroscopic probes.

EXPERIMENTAL SECTION

Materials. The amide form of the N-terminal icosapeptide amyloid-β (Aβ_{1-20}) was synthesized at the University of South Florida Peptide Synthesis and Mass Spectrometry Center, and the accuracy and purity verified with MALDI-TOF and HPLC. The flavonoids (Figure 1) quercetin (Qr), myricetin (Mr), 3-hydroxyflavone (3Hf), 5-hydroxyflavone (5Hf), (+)-catechin (Ct), and (−)-epicatechin (Et), catechol, and dopamine and other chemicals of the highest purity were acquired from commercial sources and were used as received (Sigma-Aldrich, St. Louis, MO). Metal chloride salts or metal atomic absorption standards were used for the preparation of metal complexes of the peptide and flavonoids (Fisher Scientific, Pittsburgh, PA). Deionized water (18 MΩ) was obtained from a Millipore Milli-Q system. Plastic ware and glassware were demetallized with EDTA and extensively rinsed. All solutions were freshly prepared just prior to the experiments. Triethylamine (TEA) was added in some cases to deprotonate the ligands for metal binding. In a typical metal-binding study monitored by NMR, TEA was titrated into a 1:1 metal-to-flavonoid sample in 0.1 equivalent increments until the integrations of diamagnetic and paramagnetically shifted proton signals become approximately equal for performing optimal saturation-transfer experiments. Such titration can also selects for a preferential metal-binding site of the flavonoid.

Kinetic Studies. The CuAβ_{1-20} complex was prepared as previously described.[11,17] The oxidation of a substrate by CuAβ_{1-20} in the presence or absence of H_2O_2 was monitored in 100 mM HEPES at pH 7.0 and 25 °C with the *o*-quinone indicator MBTH present in equal amounts as the substrate during the assay.[41] Formation of the quinone product was tracked photometrically (ε = 27,200 M^{-1} cm^{-1} for dopamine,[42] 32,500 M^{-1} cm^{-1} for catechol,[42] and 10,040 M^{-1} cm^{-1} for Ct and Et[43] at 500 nm) with a Varian CARY 50 spectrophotometer (Varian, Palo Alto, CA) equipped with a Water Peltier PCB-150 thermostable cell. The molar absorptivity values of oxidized flavonoids were determined by means of the tyrosinase assay,[44] wherein the flavonoids with known concentration were subjected to oxidation by tyrosinase in the presence of 100 mM H_2O_2, and the formation of the corresponding *o*-quinones were monitored by the use of MBTH until the reactions reach completion. The rate constants k_{cat} and $K_m = (k_{cat} + k_{-1})/k_1$ in pre-equilibrium kinetics analogous to the Michaelis−Menten kinetics are determined by fitting the data to eq 1,

$$\text{rate} = k_{cat}[\text{CuA}\beta]_o[S]_o/(K_m + [S]_o) \quad (1)$$

where S is the substrate and K_m is the Michaelis constant. Inhibition of the reaction was performed under similar conditions, with various concentrations of an inhibitor to reveal the inhibition pattern and determine the inhibition constant K_I. The effect of Ca^{2+} (or Yb^{3+}) on Qr inhibition against CuAβ activity was performed similarly with various amounts of Ca^{2+} and the rates of oxidation determined in the presence of a certain amount of Qr. All the kinetic constants were obtained via nonlinear fittings, whereas some results are plotted in linear manner for clarity.

Spectroscopic Studies. The electronic spectra were obtained with the Cary 50 spectrophotometer. For metal-binding studies, 20 μM of Qr was titrated with a metal ion solution in DMSO, and the absorptions corresponding to metal−Qr complex formation were monitored. DMSO is a convenient solution to the low solubility of flavonoids, allowing for more accurate and less noisy data in spectroscopic studies. The electronic spectra of the complexes in DMSO and buffer solutions are the same, indicating the validity of using DMSO as a convenient solvent in the studies. Moreover, the lack of exchangeable protons in DMSO also allows clear detection of solvent exchangeable paramagnetically shifted hydroxyl proton NMR signals in the Co^{2+} and Yb^{3+} complexes (see below). An optical Job plot[45] can be utilized for revealing the metal-to-ligand stoichiometry and has previously been demonstrated useful for the determination of complex metal-drug binding stoichiometry.[46] In the plot, the

dx.doi.org/10.1021/ic301832p | *Inorg. Chem.* 2013, 52, 679−690

absorption of the complex as a function of metal mole fraction (X_M) or ligand mole fraction (X_L) was obtained with a constant total concentration of metal and ligand ([M] + [L]), in which the ratio of X_M:X_L at the maximum absorption in the plot reflects the stoichiometry of the M−L complex in solution.

1D and 2D ^{1}H NMR spectra of samples at ∼2−5 mM in deuterated DMSO were acquired on a Varian INOVA500 spectrometer (at 500 MHz ^{1}H resonance) with a 5 mm biotriple resonance probe. A 90° pulse (∼6.0 μs) was used for the acquisition of 1D ^{1}H NMR spectra with 8 K data points, whereas 1024 × 512 data points were used for 2D EXSY (EXchanged SpectroscopY) experiments, with a presaturation pulse for solvent suppression. The superWEFT solvent suppression technique[47] was used in 1D spectral acquisition of paramagnetic metal−Qr complexes to suppress signals from the solvent and diamagnetic protons of relatively longer relaxation times. In a 1D ^{1}H NMR saturation transfer experiment, a selected paramagnetic proton signal was saturated with a presaturation pulse and the diamagnetic exchange counterpart was revealed by the difference spectrum between the irradiated and the reference spectra obtained by irradiating at a signal-free region near the signal of interest using identical experimental parameters. A line-broadening of 40 Hz was applied to improve the signal-to-noise ratio of the paramagnetically shifted signals. The spin−lattice relaxation times (T_1) for the paramagnetically shifted signals were determined by the use of the inversion−recovery method (D1−180°−τ−90°), with a D1 delay sufficiently long for paramagnetically shifted signals to fully relax but short for diamagnetic signals in order to reduce the total recycle time. Different experiments with various D1 values may be needed to cover the wide range of relaxation times of paramagnetic signals. The peak intensities versus the delay τ values were fitted with a three-parameter fitting program on the spectrometer to afford the T_1 values.

RESULTS

Oxidative Activity of CuAβ Toward Flavanols. Copper(II) complexes of Aβ_{1-40} and their 1−16 and 1−20 fragments exhibit similar and significant oxidative activities, effectively catalyzing oxidation of catechol, the hydroxylation of phenols, and similar reactions of several catecholamine neurotransmitters at pH 7.0 and 25 °C.[11,17] Many flavonoids contain a catechol moiety (Figure 1) and are thus expected to be oxidized by CuAβ_{1-20}. Indeed, both Ct and Et are effectively oxidized by CuAβ_{1-20} aerobically to yield *o*-quinone, with rate constants k_{cat} = 1.01 × 10^{-2} and 1.55 × 10^{-3} s^{-1}, K_m = 0.94 and 0.55 mM, and catalytic efficiency k_{cat}/K_m = 10.7 and 2.82 M^{-1} s^{-1}, respectively, at pH 7.0 and 25 °C (Figure 2A and Table 1). The oxidations of catechol and derivatives by CuAβ_{1-20} follow a dinuclear metal-centered chemistry presumably through a (CuAβ)$_2$ dimer.[11,17] In this mechanism, a di-Cu^{2+} center catalyzes two-electron oxidation of catechol and is reduced to di-Cu^{+} in the process, which can bind O_2 in the air to form one of the several different isoelectronic forms of the highly active dicopper−oxygen intermediates (i.e., a di-Cu^{+}−oxy, di-Cu^{2+}−peroxy, or di-Cu^{3+}−oxo center) similar to that in type 3 copper oxidases like tyrosinase and its model compounds, which can also be formed from binding and deprotonation of H_2O_2 to the di-Cu^{2+} center. The intermediate can then proceed to oxidize a second substrate. The prooxidant activity of flavonoids thus can be attributed to their capability to yield a mono/di-Cu^{+} center, which upon O_2 binding can produce the active a mono-Cu-superoxo center, a di-Cu^{2+}-peroxo, or an isoelectronic metal-oxo/peroxo/superoxo center as observed in chemical model systems.[48]

CuAβ_{1-20} also exhibits peroxidation activity in the presence of H_2O_2.[17] The rates of Ct and Et oxidation by CuAβ_{1-20} are significantly enhanced in the presence of H_2O_2, affording k_{cat} = 4.48 × 10^{-2} s^{-1} (4.4-fold higher than without H_2O_2) and K_m = 1.21 mM (k_{cat}/K_m = 37.0 M^{-1} s^{-1} and 3.5-fold higher) for Ct and k_{cat} = 5.19 × 10^{-3} s^{-1} (3.3-fold higher) and K_m = 0.59 mM (k_{cat}/K_m = 8.80 M^{-1} s^{-1} and 3.12-fold higher) for Et in the presence of 30 mM H_2O_2 (Solid symbols; Figure 2A). The analysis of the reactions at different concentrations of H_2O_2 by the use of the Hanes method[49] (Figure 2B and C) reveals the intrinsic dissociation constants to be $K_{i(H_2O_2)}$ = 6.80 mM for H_2O_2−CuAβ and $K_{i(S)}$ = 0.91 mM for Ct−CuAβ and apparent dissociation constants $K_{a(H_2O_2)}$ = 10.1 mM for H_2O_2−[Ct−CuAβ] and $K_{a(S)}$ = 1.17 mM for Ct−[H_2O_2−CuAβ]. Corresponding values of 4.63 mM, 0.39 mM, 6.62 mM, and 0.69 mM, respectively, are obtained for Et.

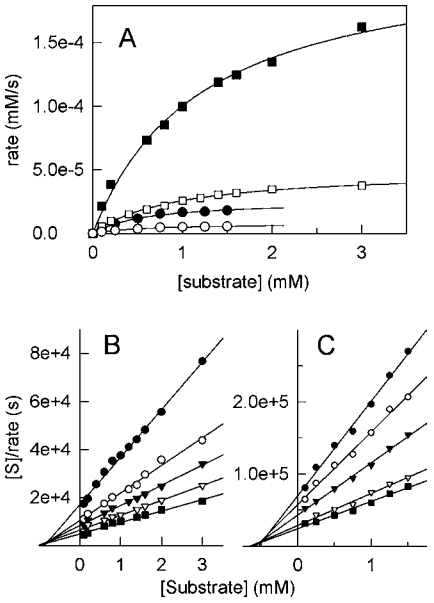

Figure 2. (A) Oxidation of Ct (square) and Et (circle) by 4.95 μM CuAβ_{1-20} with (solid symbols) and without (open symbols) 30 mM H_2O_2 and Hanes plot representation of the oxidation of Ct (B) and Et (C) by 4.95 μM CuAβ_{1-20} in the presence of (●) 2.5 mM, (○) 5.0 mM, (▼) 10.0 mM, (▽) 20.0 mM, and (■) 30.0 mM H_2O_2 in 100.0 mM HEPES at pH 7.0 and 25 °C.

Table 1. Kinetic Parameters for the Oxidation of Flavanols

S	k_{cat} (s^{-1})	$K_{m(S)}$ (mM)	$k_{cat}/K_{m(S)}$ (M^{-1} s^{-1})	$K_{(H_2O_2)}$ (mM)
Ct/air	10.1 × 10^{-3}	0.94 (0.91)[a]	10.7	(6.80)[a]
Ct/H_2O_2[b]	44.8 × 10^{-3}	1.21 (1.17)[c]	37.0	(10.1)[c]
Et/air	1.55 × 10^{-3}	0.55 (0.39)[a]	2.82	(4.63)[a]
Et/H_2O_2[b]	5.19 × 10^{-3}	0.59 (0.69)[c]	8.80	(6.62)[c]

[a]The values in parentheses are the intrinsic dissociation constants K_{iS} and $K_{iH_2O_2}$ obtained from the Hanes plots. [b]Obtained in the presence of 30 mM H_2O_2 with varying amounts of Ct or Et. [c]The values in parentheses are the apparent dissociation constants K_{aS} and $K_{aH_2O_2}$ obtained from the Hanes plots.

Inhibition of the Oxidative Activity of CuAβ by Flavonols. As opposed to the flavanols Ct and Et, the flavonols Qr and Mr (Figure 1) are not oxidized by CuAβ_{1-20} under the same conditions, despite the presence of the catechol/polyphenol moieties accessible to oxidation. Instead, they are effective inhibitors against aerobic oxidation of catechol and dopamine by CuAβ_{1-20}, with a low IC_{50} of ∼15 μM for Qr. Further kinetic analysis[49] reveals that Qr is a competitive inhibitor toward oxidation of catechol and

dx.doi.org/10.1021/ic301832p | Inorg. Chem. 2013, 52, 679−690

dopamine by CuAβ_{1-20} with K_I values of 11 and 9.5 μM, respectively (Figure 3A and C). Similarly, Mr exhibits a

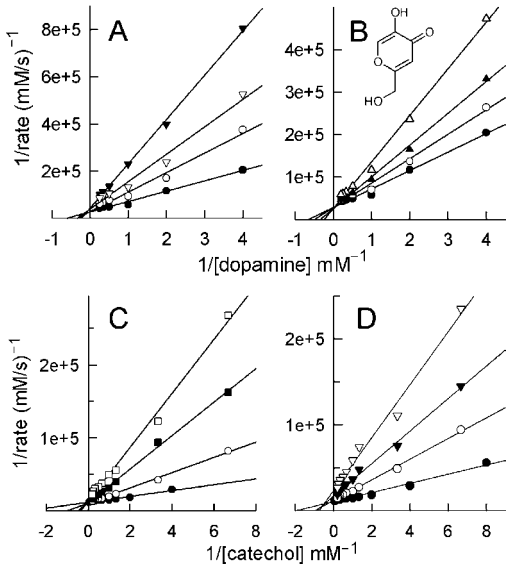

Figure 3. (A) Qr (0, 12.5, 25.0, and 35.0 μM from bottom) and (B) kojic acid (0, 10, 20, 30 mM) inhibition toward dopamine oxidation and (C) Qr (0, 25.0, 50.0, and 100.0 μM) and (D) Mr (0, 25.0, 50.0, and 100.0 μM) toward catechol oxidation by 4.95 μM Cu–Aβ_{1-20} in 100.0 mM HEPES at pH 7.0 and 25 °C.

competitive inhibition pattern toward catechol oxidation with K_I = 33 μM (Figure 3D). This competitive inhibition pattern can be attributed to their binding to the redox-active metal center of CuAβ_{1-20}. The metal-binding site in flavonols has to be a site other than the catechol moiety as catechol binding would result in its oxidation, which was not observed under our experimental conditions. The simple flavonol 3-hydroxyflavone (3Hf) has only one hydroxyl group at position 3 to form a potential metal-binding α-ketoenolate moiety (Figure 1), which inhibits catechol oxidation by CuAβ_{1-20} in a mixed-type inhibition with a competitive K_I = 16 μM for binding to CuAβ and a less significant noncompetitive inhibition constant of 57 μM for binding to the complex [catechol–CuAβ]. The mechanism of inhibition was further explored with the pyrone kojic acid (KA; 5-hydroxy-2-hydroxymethy1-γ-pyrone, shown in Figure 3B) that contains an α-ketoenolate moiety as in Qr and is a specific inhibitor toward the di-Cu oxidase/hydroxylase tyrosinase.[50] KA inhibits dopamine oxidation by CuAβ_{1-20} with K_I = 23 μM (Figure 3B). The inhibition constants of the α-ketoenolate-containing compounds are not drastically different from each other, suggesting that the inhibitory site is the α-ketoenolate moiety.

Ca^{2+}Influence. Soluble intermediate aggregates of Aβ such as protofibrils or oligomers have been proposed to destabilize cellular membranes that can contribute to a significant increase in local Ca^{2+} concentration.[51] If Qr inhibits catechol oxidation by binding to the metal center of CuAβ, the excess Ca^{2+} ions may compete for binding to these flavonols and can potentially reduce the inhibition capability of these flavonoids. Following this hypothesis, the influence of Ca^{2+} on Qr inhibition against oxidation of catechol-containing substrates was investigated. The rate of catechol oxidation by CuAβ_{1-20} inhibited by a fixed concentration of Qr increases with increasing concentration of Ca^{2+}, and a linear plot of the pre-equilibrium kinetics at various Ca^{2+} concentrations shows a competitive pattern (Figure 4A). The results indicate that the inhibitory action of Qr toward

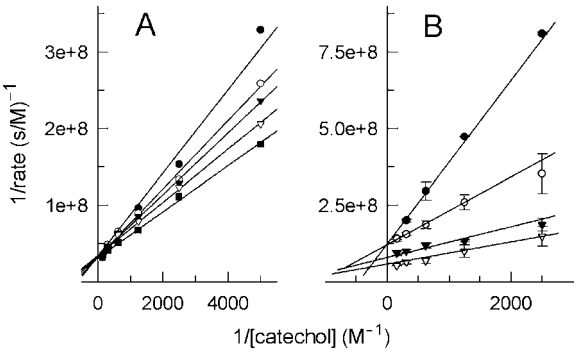

Figure 4. (A) Ca^{2+} (0, 5.0, 10.0, 20.0, and 40.0 mM from top) and (B) Yb^{3+} (0, 0.1, 0.2, 0.4, and 0.8 mM from top) influence on Qr (5.0 μM) inhibition of catechol oxidation by 3.0 μM CuAβ_{1-20} in 100 mM HEPES pH 7.0 and 25 °C.

oxidation of a catechol substrate is lessened by Ca^{2+} due to Qr binding to Ca^{2+} in competition with binding to CuAβ_{1-20}. This competition can be described by the equilibria in eq 2, from which the rate law eq 3 can be obtained, where K_I is the inhibition constant of Qr, K_m is the Michaelis constant, and K_{Ca} is the apparent dissociation constant of the Ca–Qr complex determined to be 16 ± 3 mM by fitting the rate as a function of initial Ca^{2+} concentration $[Ca]_o$ in eq 3.

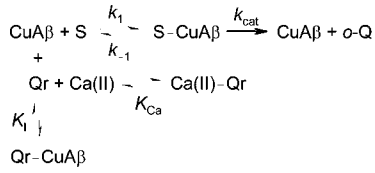

(2)

$$\nu = \frac{V_{max}[S]}{K_m\left[1 + \left(\frac{K_{Ca}[I]_o}{[Ca]_o + K_{Ca}}\right)/K_I\right] + [S]} \quad (3)$$

Quercetin Binding to Metal Ions and Cu-β-Amyloid. Because the oxidations of catechol and dopamine by CuAβ are inhibited by flavonols and the presence of Ca^{2+} reduces this inhibition effect, Qr may compete with catechol in binding to the CuAβ center. Qr has three possible metal-binding sites: β-ketophenolate, α-ketoenolate, and catecholate moieties (Figure 1). Many examples are known for metal binding to one or more of these moieties,[52] such as the preferred binding of flaviolin to the active-site metal in cytochrome P450 via the ketophenolate moiety (rather than the ketoenolate moiety)[53] and the spectroscopically characterized metal-binding to the ketophenolate site(s) of the anthracycline anticancer drugs.[46,54] Because Qr and Mr are not oxidized by CuAβ, it is possible that the catechol or the polyphenol ring B in these two flavonols does not interact with the metal center. The interactions between Qr and several metal ions were further analyzed to investigate the metal-binding possibilities. Qr shows a characteristic absorption at 383 nm in DMSO (trace a, Figure 5A) that shifts to 450 nm upon addition of Cu^{2+} (trace d, Figure 5A), as previously observed in ethanol.[55] The change in the absorption at 450 nm $\Delta\lambda_{450}$ as a function of $[Cu^{2+}]$ can be fitted to 1:1 metal-to-ligand stoichiometry to obtain an affinity constant $K_{f(Cu)}$ = (9.2 ± 6.6) × 10^5 M^{-1} (Figure 5B, ●). Furthermore, the optical Job plot for the formation of Cu^{2+}–Qr

dx.doi.org/10.1021/ic301832p | Inorg. Chem. 2013, 52, 679–690

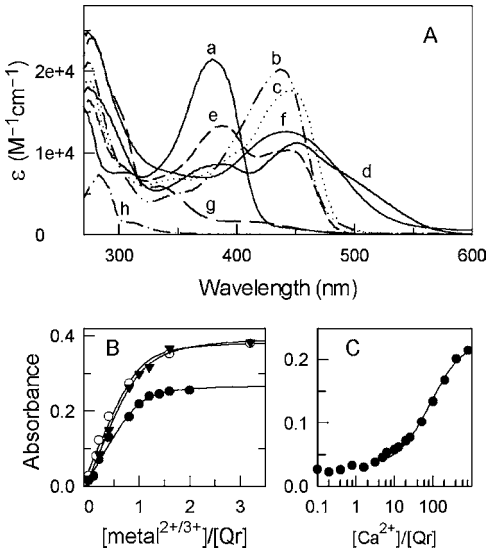

Figure 5. (A) Electronic spectra of different metal-flavonoid complexes (a, Qr; b, Yb^{3+}–Qr; c Co^{2+}–Qr; d, Cu^{2+}–Qr; e, Ca^{2+}–Qr; f, (Cu^{2+}–Aβ_{1-20})–Qr; g, Co^{2+}–5Hf; h, Co^{2+}–Ct). With the exception of the spectrum of (Cu^{2+}–Aβ_{1-20})–Qr acquired in 100 mM HEPES pH 7.0 buffer, the rest were obtained in DMSO with appropriate amount of triethylamine added as explained in the Materials section. (B) The change in absorption was fitted to 1:1 metal-to-ligand binding to obtain corresponding affinity constant for Cu^{2+} (●), Co^{2+} (○), and Yb^{3+} (▼) and for Ca^{2+} (C) in a semilog plot.

shows a maximum at X_{Cu} = 0.5 and can be fitted to 1:1 metal-to-ligand stoichiometry (Figure 6A, ■), indicating the formation of Cu^{2+}–Qr complex. Similarly, Co^{2+} binding to Qr in DMSO shows a λ_{max} at 450 nm, analogous to previously reported under various conditions[56] and Cu^{2+} binding

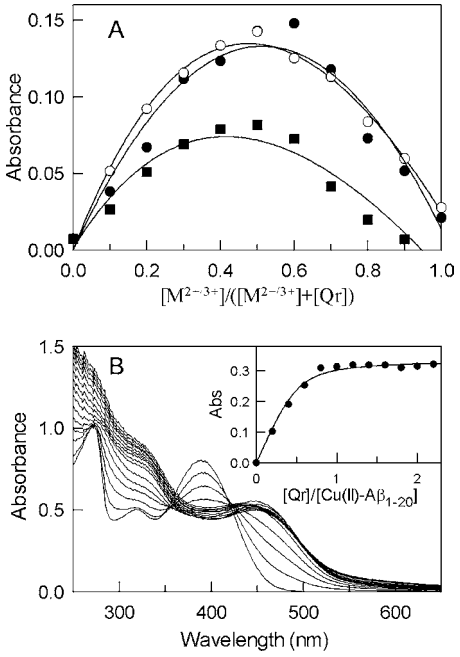

Figure 6. (A) Optical Job plots of Cu^{2+} (■), Co^{2+} (●), and Yb^{3+} (○) binding to Qr in DMSO and fitted to a 1:1 metal–Qr species. (B) Electronic spectra of Qr binding to Cu^{2+}–Aβ_{1-20} in 100 mM HEPES pH 7.0 at 25 °C and fitted to 1:1 Qr–(Cu^{2+}–Aβ_{1-20}) complex to afford $K_{Affinity}$ = (1.3 ± 0.2) × 10^7 M^{-1}.

described above, yielding the affinity constant $K_{f(Co)}$ = (4.5 ± 1.7) × 10^5 M^{-1} for Co^{2+}-to-Qr stoichiometry of 1:1 (trace c, Figure 5A; ○, B) which is also confirmed by the optical Job plot (Figure 6A, ●). The flavonoid 5-hydroxyflavone (5-Hf) has only a β-keto-phenolate metal-binding moiety, while Ct possesses only the catechol moiety for possible interaction with metal ions. The binding of Co^{2+} with 5-Hf (410 nm, Figure 5A, trace g) or with Ct (313 nm, Figure 5A, trace h) does not show the characteristic absorption at 450 nm in the Co^{2+}–Qr complex (Figure 5A, trace c), indicating the Co^{2+} binding site in Qr cannot be β-ketophenolate (as in 5-Hf) nor catecholate (as in Ct). These results indicate that the α-ketoenolate moiety is the most likely metal-binding site on Qr, which is further confirmed with NMR discussed below.

Upon addition of Qr to CuAβ_{1-20} in buffer at pH 7.0, an absorption band at 450 nm appears, consistent with those of the metal–Qr complexes described above (Figures 5A, trace f, and 6B). The absorption reaches a plateau after 1.0 equivalent of Qr (Figure 6B, inset), which can be fitted to a 1:1 complex of Qr–CuAβ_{1-20} with a significant affinity constant $K_{f(CuA\beta)}$ = (1.3 ± 0.2) × 10^7 M^{-1}, larger than that for Qr binding to Cu^{2+} ions that may be attributed to Qr interaction with Aβ peptide[57] in addition to the metal. The optical features also indicate Qr binds to the metal in Cu–Aβ via its α-ketoenolate moiety. The appearance of the absorption at 450 nm in DMSO, a pH 7.0 buffer, and ethanol[55] indicates the same metal-binding mode of Qr in the different solvents.

Because Ca^{2+} influences the inhibition properties of Qr toward catechol oxidation, the interaction of Ca^{2+} with Qr was further investigated. Addition of Ca^{2+} to Qr results in a new absorption at 450 nm, analogous to the transition metal complexes of Qr (Figure 5A, trace e). Fitting of the absorption as a function of Ca^{2+} concentration gives an affinity constant $K_{f(Ca)}$ = 580 M^{-1} (i.e., K_d = 1.7 mM). This value is much smaller than the values for other metal ions (Figure 5C), yet comparable to the reported value of 821 M^{-1} obtained by potentiometric methods.[58] Note that the normal total serum Ca^{2+} concentration is about 2 mM, and approximately 1 mM of this is free Ca^{2+},[59] comparable to the measured K_d value. However, the dissociation constant of 1.7 mM is 10-fold lower than that obtained from the kinetic measurement (K_{Ca} = 16 mM), suggesting that the latter might be an apparent dissociation constant of more than one equilibrium, such as a solvation effect from conducting the kinetic measurements in aqueous buffer. This relatively high K_d also suggests that serum Ca^{2+} cannot successfully compete with Cu–Aβ in binding to Qr and decreases the efficacy of Qr inhibition of the oxidation chemistry *in vivo*.

The lanthanides have similar radii and ligand binding preferences as Ca^{2+} and have served as spectroscopic probes to gain structural and mechanistic information about Ca^{2+} in biological systems.[60] Under this premise, Yb^{3+} was used as a probe for the investigation of Ca^{2+} binding to Qr. Titrating Yb^{3+} to a Qr solution shows an absorption at 440 nm (Figure 5A, trace b) analogous to other metal binding herein described and can be fitted to 1:1 metal-to-Qr stoichiometry with a formation constant $K_{f(Yb)}$ = (4.6 ± 0.7) × 10^5 M^{-1} (Figure 5B, ▼). This value is comparable to La^{3+} binding (8.3 × 10^5 M^{-1}, which was suggested to form a 1:3 complex[61]) yet much higher than that for Ca^{2+} binding (Figure 5C) presumably due to its higher charge. The formation of a predominant 1:1 metal-to-ligand complex is confirmed with an optical Job plot by showing a maximum at X_{metal} ~ 0.5 under the experimental

dx.doi.org/10.1021/ic301832p | *Inorg. Chem.* 2013, 52, 679–690

conditions (Figure 6A, ○), despite the preferred high coordination number of ≥7 for lanthanide ions.[60] Depending on the solution conditions, low ratios of ligand-binding stoichiometry were observed for lanthanide binding to anthracycline drugs.[46] Like Ca^{2+}, Yb^{3+} can also significantly influence Qr inhibition, showing a competitive pattern at low concentrations but noncompetitive pattern at higher concentrations probably attributed to nonspecific interactions with the Aβ peptide and/or the substrate at higher concentrations. A much lower dissociation constant K_{Yb} = 0.11 ± 0.01 mM is obtained compared to that of Ca^{2+} (K_{ca} = 16 ± 3 mM in eqs 2 and 3) from kinetic studies. The intrinsic Yb^{3+} dissociation constant $1/K_{f(Yb)} = 2.2 \times 10^{-6}$ M of Yb−Qr is much smaller than the kinetic dissociation constant, once again suggesting the presence of more than one equilibrium for Yb^{3+} binding in kinetic measurements.

^{1}H NMR of Paramagnetic Co^{2+}− and Yb^{3+}−Qr Complexes. The slow electronic relaxation of Cu^{2+} can broaden NMR signals of nearby protons beyond detection, whereas high-spin Co^{2+} with fast-relaxing electrons has been used as a paramagnetic probe for the study of the metal coordination environments in metalloproteins and complexes.[62] The ^{1}H NMR spectrum of Co^{2+}−Qr acquired in d_6-DMSO displays 8 (out of 10 protons on Qr) hyperfine-shifted signals within a region between 60 to −80 ppm, including OH signals that are not in exchange with DMSO (Figure 7A). A recently reported ^{1}H NMR spectrum of a Co^{2+}−Qr complex concluded to have all signals corresponding to the complex in the diamagnetic region.[56] This observation is not consistent with the paramagnetism of Co^{2+} and can be attributed to dissociation of the complex or the complex became diamagnetic with a Co^{3+} center under the conditions the study was performed. Likewise, the ^{1}H NMR spectrum of a Cu^{2+}−Qr complex was reported to have clear signals in the diamagnetic region.[63] This is inconsistent with the significant paramagnetic relaxation of Cu^{2+}, which would render the NMR signals too broad to be clearly detected/assigned.[62] In another study, a (3-Hf)-bound ternary complex of Co^{2+} shows well-resolved hyperfine-shifted signals;[64] however, the signals due to 3-Hf were not assigned in order to compare with the corresponding signals in Co^{2+}−Qr.

A complete assignment of the hyperfine-shifted ^{1}H NMR signals of the Co^{2+}−Qr complex can be accomplished by the use of 1D and 2D EXSY saturation transfer NMR techniques, owing to the presence of fast exchange between the bound and free forms of Qr under the equilibrium Co^{2+} + Qr ⇌ Co^{2+}−Qr. Solvent exchangeable OH signals are identified at 17.0, 16.3, and −75.1 ppm, which disappear upon addition of a few drops of D_2O to the DMSO solution. The five less-shifted signals of the complex are connected to their counterparts of the free ligand in the EXSY spectrum (Figure 8 and Table 2), in which signals at 17.0 and 16.3 ppm can be assigned to the 3′-OH and 4′-OH protons, respectively, of the catechol moiety, while the remaining three signals are due to 6-H, 8-H, and 5′-H protons. The three farthest shifted signals with short relaxation times <10 ms are assigned with 1D saturation transfer experiments. Irradiation of the signal at −75.1 ppm reveals saturation transfer to the signal at 12.5 ppm assigned to 5-OH, and the signals at 56.4 and 49.8 ppm are associated with 6′-H and 2′-H protons, respectively (Figure 9, Table 2).

Yb^{3+} was also used as a paramagnetic probe[62] to gain metal binding of Qr via a complete assignment of the hyperfine-shifted ^{1}H NMR signals of the Yb^{3+}−Qr complex. The ^{1}H NMR spectrum of the complex displays eight paramagnetically shifted signals in the range of 20 to −40 ppm (Figure 10), of which the signals at 19.2, 8.8, and 2.1 ppm are solvent exchangeable OH signals. From the EXSY spectrum, seven hyperfine-shifted signals of the complex can be correlated to their diamagnetic counterparts of metal-free Qr and assigned

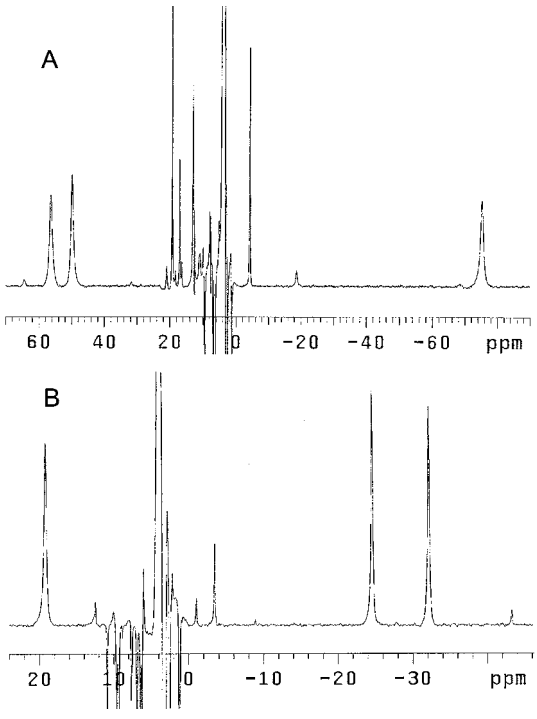

Figure 7. ^{1}H NMR spectrum of Co(II)−Qr complex (A) in the presence of 1.5 equivalent of triethylamine in d_6-DMSO. In the absence of TEA, only weak Co(II) binding by Qr was observed and Yb(III)−Qr complex (B) in the presence of 0.7 equivalent of TEA in d_6-DMSO acquired as in (A). The different signal intensities and phases are attributable to their very different relaxation times, wherein the slowly relaxing protons are significantly suppressed by the super-WEFT pulse sequence.

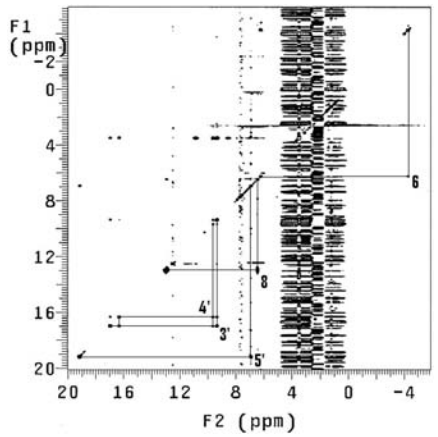

Figure 8. The 2D ^{1}H EXSY spectrum of the 1:1 Co^{2+}−Qr complex in d_6-DMSO, acquired with a mixing time of 89.3 ms. The paramagnetic signals of the complex are correlated to their diamagnetic counterparts, and the numbers next to the crosspeaks represent the protons according to figure 1. The few far-shifted fast-relaxing signals are correlated with 1D saturation transfer techniques shown in Figure 9.

dx.doi.org/10.1021/ic301832p | Inorg. Chem. 2013, 52, 679−690

Table 2. Assignment of the Hyperfine-Shifted ^{1}H NMR signals of the 1:1 Co^{2+}−Qr and Yb^{3+}−Qr complexes in DMSO and Their Corresponding T_1 Relaxation Times and Calculated Distances from the Paramagnetic Center (r_{M-H})

			Co^{2+}−Qr		Yb^{3+}−Qr	
	σ_d[a] ppm	σ_p[a] ppm	r_{M-H}[b] Å	T_1 (r_{Co-H})[c] ms (Å)	σ_p ppm	T_1 (r_{Yb-H})[c] ms (Å)
6′-H	7.5	56.4	6.60 (6.49; 6.44)[d]	5.4 (4.19)	−32.2	24 (4.44)
2′-H	7.6	49.8	4.10 (3.65; 4.24)[d]	6.2 (4.28)	−24.6	32 (4.66)
5′-H	6.9	19.1	8.07 (7.86; 8.20/5.92)[e]	89 (6.68)	−3.5	339 (6.90)
3′−OH	9.3	17.0	NA (6.19; 7.18/9.50)[e,f]	213 (7.72)	2.1	638 (7.67)
4′−OH	9.6	16.3	NA (8.67; 9.30)[f]	408 (8.61)	4.1	ND
8-H	6.4	13.0	7.24 (7.64; 7.38)	158 (7.35)	−1.1	554 (7.49)
6-H	6.2	−4.3	7.04 (8.16; **7.15**)[g]	134 (7.15)[g]	6.0	420 (7.15)[g]
5-OH	12.5	−75.1	NA (6.20; 4.78)[f]	4.0 (3.98)	19.2	8.3 (3.71)
7-OH	10.9	ND	NA (9.93; 9.32)[f]	ND	8.8	832 (8.01)
3-OH	9.4	ND			ND	

[a]Chemical shifts of paramagnetically shifted signals (σ_p) of the complexes and free ligand (σ_d) [b]The values are metal−proton distances from the crystal structure of a Co−flavonol complex.[64] The first values in parentheses are those from the crystal structure of a metal-bound Qr in Qr-2,3-dioxygenase via the α-ketoenol moiety,[74] and the second values in the parentheses are the distances with the metal manually moved to the position to be chelated by the α-ketoenolate moiety coplanar with Qr and with a torsion angle of 26° between rings B and C as seen in the Co−flavonol complex. [c]Metal−H distances in parentheses are derived from relaxation times. [d]The values are from the conformation in the crystal structure, wherein the positions of 2′ and 6′ protons are switchable with each other with a free rotating 2C−1′C bond determined by NMR herein. [e]The two values are the maximal and minimal values due to a free rotating 2C−1′C bond. [f]An estimated average value due to a free-rotating C−O bond. [g]This proton is used as the reference for M−H distances.

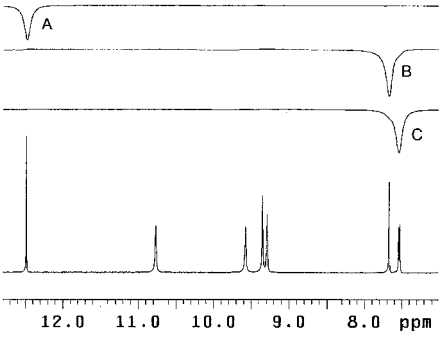

Figure 9. Typical 1D ^{1}H saturation−transfer difference spectra of the 1:1 Co^{2+}−Qr complex show saturation transfer from irradiated hyperfine-shifted signals at −75.1, 49.8, and 56.4 ppm to their corresponding diamagnetic protons at 12.5 (A), 7.6 (B), and 7.5 (C) ppm. The broadness in the difference spectra A−C is due to the application of a line-broadening window function of 30 Hz.

(Table 2). The remaining hyperfine-shifted signal at 6.0 ppm is assigned by 1D saturation transfer to the 6-H proton at 6.2 ppm.

DISCUSSION

Flavonoids are very effective antioxidants, presumably attributed to their readily oxidizable (poly)phenol moieties.[20−22] As a result, they serve as suicide antioxidants and compete with and protect oxidation-sensitive biomolecules by binding/interacting with oxidizing agents. In the process, they are oxidized in place of biomolecules, thus serving a protective role. Conversely, pro-oxidant activities of flavonoids have been reported.[23] The results presented here indicate that the antioxidation mechanism of flavonols (Qr and Mr) against the oxidative activity of CuAβ is different from that of flavanols (Ct and Et). The flavanols are simply substrates (Figure 2A) whereas the flavonols are competitive inhibitors (Figure3A, C, and D), despite the presence of easily oxidized catechol or polyphenol moieties. Although flavonoids are generally recognized to exhibit broad health benefits as antioxidants[20−22] and potential signaling molecules,[24] their antioxidation mechanisms toward

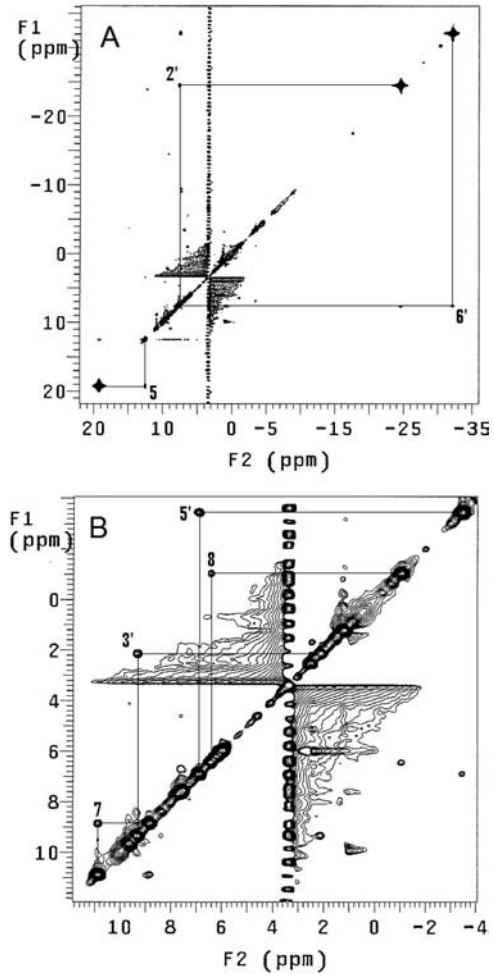

Figure 10. (A) 2D ^{1}H EXSY spectra of 1:1 Yb^{3+}−Qr complex in d_6-DMSO, acquired with a short mixing time of 8.3 ms that enables detection of all exchange pairs in the spectral window of ~55 ppm. (B) Enlarged near-diamagnetic region of the spectrum in (A).

dx.doi.org/10.1021/ic301832p | Inorg. Chem. 2013, 52, 679−690

metal-mediated redox chemistry have not been well correlated to metal-binding or interaction. Understanding how they interaction with metal ions and correlating how they react as antioxidants is important for better design of metal-binding antioxidants for medicinal purposes.

Quantitative Analyses of Different Types of Antioxidation of Flavonoids Against Cu−Aβ. The antioxidation mechanism observed for Ct and Et can be described by eq 4 with two parallel reactions, one for the substrate and the other for the flavanols that serve as suicide substrates to compete for binding to the redox-active metallo−Aβ. The rate law can be derived on the basis of steady-state approximation (eq 5), wherein $K' = (k'_{cat} + k'_{-1})/k'_1$, which describes the initial rate of the oxidation of the substrate S1 (such as a catecholamine neurotransmitter) in the presence of an antioxidant S2 (such as Ct). Thus, the smaller the K' value of an antioxidant, the better it can serve as an inhibitor against the oxidative activity of CuAβ. If S2 is not oxidized, as the case of Qr (i.e., $k'_{cat} = 0$), a standard competitive inhibition rate law is applicable with K' being the inhibition constant K_i.

$$\mathrm{CuA}\beta \begin{cases} +\mathrm{S1} \underset{k_{-1}}{\overset{k_1}{\rightleftarrows}} \mathrm{S1-CuA}\beta \xrightarrow{k_{cat}} \mathrm{prod1} \\ +\mathrm{S2} \underset{k'_{-1}}{\overset{k'_1}{\rightleftarrows}} \mathrm{S2-CuA}\beta (\xrightarrow{k'_{cat}} \mathrm{prod2}) \end{cases} \quad (4)$$

$$\mathrm{rate} = \frac{k_{cat}[\mathrm{CuA}\beta]_0[\mathrm{S1}]}{K_m\left(1 + \frac{[\mathrm{S2}]}{K'}\right) + [\mathrm{S1}]} \quad (5)$$

Because of the fast oxidation rates of Ct and Et, their "inhibitions" against catechol or dopamine oxidation by acting as suicide substrates cannot be evaluated in the same way as regular inhibitors such as Qr and Mr. Nevertheless, their antioxidation efficacies can be quantitatively evaluated once their rate constants as substrates are obtained. For example, the presence of 112 μM Qr, 10-fold higher than its K_i, would decrease the rate of dopamine oxidation $(\mathrm{rate}_o - \mathrm{rate}_i)/\mathrm{rate}_o$ by 90% at [dopamine] ≪ K_m (0.90 mM[17]). However, under the same conditions, 112 μM Ct with K_m = 0.94 mM would decrease the rate of dopamine oxidation by only ∼6%. Moreover, Ct and Et are oxidized at the same time serving as antioxidants which further decreases their effective concentrations with time.

Regioselective Oxidation. Although both Ct and its stereo isomer Et are effectively oxidized by Cu−$A\beta_{1-20}$, different reaction rates and specificities are observed. Their relative aerobic oxidation turnover rates and catalytic efficiencies are $k_{cat(Et)}/k_{cat(Ct)}$ = 15% and $(k_{cat}/K_m)_{Et}/(k_{cat}/K_m)_{Ct}$ = 27% respectively, Et is also more resistant to peroxidation by 30 mM H_2O_2 relative to Ct, i.e., 11.6% and 23.8%, respectively. Owing to its lower K_m values than those of its isomeric counterpart Ct in the presence and absence of H_2O_2, Et is a better antioxidant than Ct in terms of kinetics, cf. eq 5. Moreover, the much higher k_{cat}/K_m value for Ct oxidation makes it a better substrate for oxidation reactions and thus is more effectively consumed and becoming less inhibitory than Et with time. The resistance to oxidation and the competitive inhibition pattern of Qr and Mr indicate that neither of these two flavonoids binds to the active metal center of CuAβ through the catechol/polyphenol C ring nor do they remove the metal from CuAβ, which would result in noncompetitive inhibition pattern[49] due to the decrease in the concentration of the catalytic center.

Interactions with Cu−Aβ. A few flavonoids have been demonstrated to inhibit formation of amyloid fibrils.[37] A recent study showed that Mr at 50 μM can decrease metal-mediated aggregation and protect neuroblastoma cells against neurotoxicity of Aβ at 25 μM.[65] Because Mr and Qr bind to but do not remove the metal from Cu−amyloid on the basis of the kinetic studies shown here, other interactions and/or molecular properties of the flavonol−metallo−Aβ ternary complex have to be involved in the above observations. Binding of flavonol to the metal center of CuAβ would introduces polyphenol hydroxyl groups to the peptide for potential hydrophilic interactions. Direct comparison of our kinetic studies with the above observation cannot be made at this stage owing to the different experimental conditions, e.g., the lower concentrations and shorter experimental time period in the kinetic studies. Future investigation about the effects of flavonoids and polyphenols toward the structure and chemistry of metallo−Aβ can be expected to provide clues for design of specific molecules against this neurotoxic metallopeptide.

Metal Binding to Flavonols. Qr has three possible metal-binding sites (Figure 1): (a) the β-ketophenolate on ring A, (b) the α-ketoenolate on ring C, and (c) the catechol moiety on ring B. The catechol and the β-keto-phenolate moieties have pK_a values in the range of 9.4−13.4 and 11−12, respectively; whereas the pK_a value of the α-ketoenolate moiety is estimated to be 13−15.5.[66]On the basis of their pK_a values, the metal can be expected to successfully compete with proton and bind preferably at either the catechol or the β-ketophenolate site which loses proton(s) more easily, consistent with the $Al(Qr)_2$ complex based on solid-state ^{13}C NMR study.[67] The crystal structures of metal−3Hf complexes[68] and a few ternary metal complexes[64,69] of 3Hf revealed a metal-bound 3Hf via the α-ketoenolate moiety. However, the α-ketoenolate moiety in 3Hf is the only metal-binding group in these complexes, thus the metal-binding preference cannot be revealed in these complexes. Moreover, the natural product flaviolin (4,5,7-trihydroxynaphthalene-1,2-dione) binds to the active-site metal in cytochrome P450 A158A2 via the ketophenolate moiety rather than the enolate moiety,[70] reflecting potentially complicated binding of Qr with metal ions and metallo−Aβ owing to the three different metal-binding sites.

Metal complexes of flavonols exhibit various metal-to-ligand ratios of 1-to-1, 1-to-2, 1-to-3, and 2-to-1 under various conditions.[55,61,63,71] Our results show that Co^{2+} binding to Ct or 5-Hf has different electronic absorptions from its binding to Qr (Figure 5A), suggesting different metal binding modes among these flavonoids, and that the α-ketoenolate site is the preferred metal-binding site on Qr. A few flavonols including Qr are competitive inhibitors toward di-Cu tyrosinase,[72] in which they are proposed to bind to the di-Cu active site via the α-ketoenolate moiety. This is probably the site for Qr binding to CuAβ, which has been suggested to follow a dinuclear oxidation pathway[11,17] analogous to catechol oxidase and tyrosinase mechanisms.

Paramagnetic NMR for Structure Determination. For better understanding of the beneficial effects of flavonoids toward AD and oxidative-stress-related disorders, their detailed molecular properties and interactions with redox-active metal centers must be clearly revealed. The 5-OH proton in the Co^{2+} and Yb^{3+} complexes with large NMR hyperfine shifts and short relaxation times (Table 2) reflects its proximity to the bound paramagnetic metal ion,[62] consistent with metal binding to the α-ketoenolate moiety. Conversely, the small hyperfine shifts

dx.doi.org/10.1021/ic301832p | Inorg. Chem. 2013, 52, 679−690

and long relaxation times of the 3′-OH and 4′-OH protons on the B-ring exclude the catechol moiety from metal binding observed previously at alkaline conditions.[73] Because of high Lewis acidity of the metal ions, these catechol hydroxyl groups should deprotonate and lose paramagnetically shifted ^{1}H NMR signals if Co^{2+} or Yb^{3+} would bind to the catechol moiety. In addition, the large chemical shifts and short T_1 values of the 2′-H, and 6′-H protons reflect their close proximity to the paramagnetic center, consistent with the α-ketoenolate moiety being the metal-binding site. The similar T_1 values of 2′-H and 6′-H protons reflect that ring B is either in free rotation with respect to ring C or is near perpendicular to ring C. Moreover, the signal for 3-OH has remained unaccounted for after all the paramagnetically shifted signals for the Co^{2+}− and Yb^{3+}−Qr complexes are assigned, which indicates that 3-O^- is involved in metal-binding.

In paramagnetic systems, the T_1 relaxation time of a hyperfine-shifted signal is proportional to the sixth power of the distance between the corresponding proton and the paramagnetic center r_{M-H}.[6,62] Thus, relative distances of protons from the metal center can be determined with respect to a rigid proton whose distance can be better estimated such as 6-H. The bound Qr in quercetin 2,3-dioxygenase (QD)[74] is coordinated to the metal with two very different Cu−O bond lengths (i.e., 2.28 Å to O-keto and 3.39 Å to O-enolate) and has off-planar Cu-binding (by ∼55°), and a planar structure; whereas the metal−flavonol complexes have about equal (∼2.0 Å) metal−O bond lengths, in-plane Cu binding, and ∼25° rotation of ring B which afford a shorter Cu−6H than Cu−8H distance. The structures of metal−Qr complexes are expected to be closer to that of the simple metal−flavonone complexes, which can serve as models along with the bound Qr in the Qr−QD structure to afford metal−H distances (Table 2, footnote b). Taking the Cu−(6-H) distance of 7.15 Å from the modified structure and the measured T_1 values of 134 and 420 ms of 6-H in the Co^{2+} and Yb^{3+} complexes, respectively, as the references, distances of all other protons to the metal center can be determined as $7.15 \times (T_1/134)^{1/6}$ in Co−Qr and $7.15 \times (T_1/420)^{1/6}$ in Yb−Qr (Table 2). The results are consistent with metal binding through the α-ketoenolate site as far as the rigid 8-H is concerned. The short distances to the metal center for the 6′-H and 2′-H protons reflect a fast free rotation between rings B and C. The structures of the Co/Yb−Qr complexes in solution are more analogous to those of the simple metal−flavonol complexes than the metal−Qr moiety in Qr−QD. A theoretical study of the structure and electronic spectroscopic features of Cu−Qr by means of density functional theory (DFT) also suggested the α-ketoenolate site to be the preferred Cu-binding site.[75]

Implication in Ca^{2+} Regulation. A common occurrence among neurodegenerative diseases is the dysfunction of mitochondria, which affects its function in Ca^{2+} modulation and leads to influx of intracellular Ca^{2+} ions.[76] Apart from oxidative stress, interference in cellular Ca^{2+} homeostasis by Aβ was also suggested to contribute to AD pathology.[77] Aβ can span the cell membrane that creates ion channels[78] and causes membrane depolarization and impair Na^+/K^+-ATPase,[79] leading to an increase in Ca^{2+} influx.[80] The rise in the Ca^{2+} level may defect neurons and synapses, deter long-term potentiation in certain brain regions, and lead to impairments in learning and memory.[81] Thus, maintaining Ca^{2+} homeostasis in the brain is also essential toward the treatment of AD.[82] Qr and/or Mr can participate in many Ca^{2+}-associated biological processes and activities, including (a) maintaining the Ca^{2+} homeostasis in the brain of D-galactose-treated mice,[83] (b) reducing Glu-induced Ca^{2+} overload that causes neuronal cell death by caspase-3,[84] (c) protecting cells from ionophore-induced intracellular Ca^{2+} overload and delaying Ca^{2+}-dependent cell death,[85] (d) serving as an effective mast cell inhibitor for allergic and inflammatory diseases more effectively than cromolyn by decreasing interleukin-6 and cytosolic Ca^{2+} level and inhibiting NF-κ B activation,[86] and (e) exhibiting concentration-dependent relaxation of human bronchial rings contracted by acetylcholine or histamine and also inhibition of K^+ and Ca^{2+}-dependent contraction.[87] Whether or not Ca^{2+}-binding of flavonols and analogous compounds implies a possible role in buffering Ca^{2+} dysregulation and signaling in AD and other disorders may be worth further exploration.

■ CONCLUDING REMARKS

Flavonoids have been shown to exhibit therapeutic benefits toward age-related neurodegenerative diseases such as Parkinson's and Alzheimer's disease (AD).[22g,32] A broad investigation involving different ethnic groups of 23 countries suggests higher dietary consumption of flavonoids, particularly flavonols, is correlated with lower population rates of dementia.[88] The results presented in this report regarding the metal-binding capability and the inhibitory effect (rather than simply serving as antioxidants and being oxidized) of the flavonols Qr and Mr toward the oxidative chemistry of CuAβ support their further use as molecular templates for drug design and finding strategies for potential prevention/treatment of oxidative stress in AD and other disorders. Because Qr can widely distribute in the body[19] (yet to a smaller extent in the brain) and exhibit positive beneficiary effects in animal models with neuronal disorders,[32,33] such as cerebrovascular insults, design of flavonols capable of passing through the blood-brain barrier in a tunable manner may lead to new directions for combating AD and other neurodegenerative disorders. The results herein conclusively reveal that Qr can form primarily a 1:1 complex with Co^{2+}, Cu^{2+}, Ca^{2+}, or Yb^{3+} ions and Cu−Aβ in solutions through the α-ketoenolate moiety. This moiety plays the key role in the flavonol family to exhibit competitive antioxidation activity against metal-mediated oxidative reactions, in sharp contrast to the suicide antioxidative flavanols Ct and Et that are easily oxidized and lose efficacy with time. Oxidative stress was found to precede fibril deposition of Aβ_{1-42} in transgenic animal models *C. elegans*[89] and mice[90] and also occurs early in AD progression prior to the development of the pathologic hallmarks Aβ plaques and tau tangles in the brains of Down's syndrome, sporadic AD, and familial AD patients.[2,91] Thereby, inhibition of the oxidation chemistry of metallo−amyloid and other potential redox centers by dietary flavonoids and analogous compounds may be a useful strategy for AD prevention. The metal-binding capability of the flavonols Qr and Mr may play a dual role in preventing further damages resulted from oxidative stress by acting as an inhibitor toward the oxidation reaction and as a regulator for biological buffering of metal ions. Moreover, Cu−Aβ shows 8.6- and 4.2-fold regioselective peroxidation of Ct over Et in terms of first- and second-order rate constants k_{cat} and k_{cat}/K_m, respectively, suggesting potential future developments and applications in regioselective catalyzes by metallopeptides.

dx.doi.org/10.1021/ic301832p | *Inorg. Chem.* 2013, 52, 679−690

AUTHOR INFORMATION

Corresponding Author

*E-mail: ming@usf.edu.

Present Addresses

[†]Department of Chemistry, University of Illinois at Chicago, 845 W. Taylor St., 5305 SES, Chicago, Illinois 60607, United States

[‡]Department of Biochemistry & Cell Biology, Rice University, Houston, Texas, United States

Notes

The authors declare no competing financial interest.

ACKNOWLEDGMENTS

Our work on metallopeptide chemistry has been supported by the National Science Foundation (CHE-0718625). Dr. Mohanraja Kumar of the Peptide and MS Center at the University of South Florida is acknowledged for the syntheses and characterizations of the peptides used herein.

DEDICATION

In memory of Professor Ivano Bertini, whose "paramagnetic NMR" explorations enlightened our research endeavors. W.M.T. dedicates this work to his beloved grandfather who suffered from Alzheimer's disease.

REFERENCES

(1) (a) Hardy, J.; Selkoe, D. J. *Science* **2002**, *297*, 353−356. (b) Bush, A. I. *Trends Neurosci.* **2003**, *26*, 207−214. (c) Yankner, B. A.; Lu, T. *J. Biol. Chem.* **2009**, *284*, 4755−4759.

(2) Castellani, R. J.; Smith, M. A. *J. Pathol.* **2011**, *224*, 147−152.

(3) De Strooper, B.; Saftig, P.; Craessaerts, K.; Vanderstichele, H.; Guhde, G.; Annaert, W.; Von Figura, K.; Van Leuven, F. *Nature* **1998**, *391*, 387−390.

(4) Vassar, R.; Bennett, B. D.; Babu-Khan, S.; Kahn, S.; Mendiaz, E. A.; Denis, P.; Teplow, D. B.; Ross, S.; Amarante, P.; Loeloff, R.; Luo, Y.; Fisher, S.; Fuller, J.; Edenson, S.; Lile, J.; Jarosinski, M. A.; Biere, A. L.; Curran, E.; Burgess, T.; Louis, J.-C.; Collins, F.; Treanor, J.; Rogers, G.; Citron, M. *Science* **1999**, *286*, 735−741.

(5) Davis, C. H.; Berkowitz, M. L. *Biophys. J.* **2009**, *96*, 785−797.

(6) Wakabayashi, M.; Okada, T.; Kozutsumi, Y.; Matsuzaki, K. *Biochem. Biophys. Res. Commun.* **2005**, *328*, 1019−1023.

(7) Marchesi, V. T. *Proc. Natl. Acad. Sci. U.S.A.* **2005**, *102*, 9093−9098.

(8) Evin, G.; Zhu, A.; Holsinger, D.; Masters, C. L.; Li, Q. *J. Neurosci. Res.* **2003**, *74*, 386−392.

(9) Evin, G.; Weidemann, A. *Peptides* **2002**, *23*, 1285−1297.

(10) Furlan, S.; Hureau, C.; Faller, P.; La Penna, G. *J. Phys. Chem. B* **2010**, *114*, 15119−15133.

(11) (a) da Silva, G. F. Z.; Tay, W. M.; Ming, L.-J. *J. Biol. Chem.* **2005**, *280*, 16601−16609. (b) da Silva, G. F. Z.; Lykourinou, V.; Angerhofer, A.; Ming, L.-J. *Biochim. Biophys. Acta, Mol. Basis Dis.* **2009**, *1792*, 49−55.

(12) (a) Scott, L. E.; Orvig, C. *Chem. Rev.* **2009**, *109*, 4885−4910. (b) Rauk, A. *Chem. Soc. Rev.* **2009**, *38*, 2698−2715. (c) Bonda, D. J.; Lee, H.-g.; Blair, J. A.; Zhu, X.; Perry, G.; Smith, M. A. *Metallomics* **2011**, *3*, 267−270. (d) Pithadia, A. S.; Lim, M. H. *Curr. Opin. Chem. Biol.* **2012**, *16*, 67−73.

(13) Lovell, M. A.; Robertson, J. D.; Teesdale, W. J.; Campbell, J. L.; Markesbery, W. R. *J. Neurol. Sci.* **1998**, *158*, 47−52.

(14) Bush, A. I.; Pettingell, W. H.; Multhaup, G.; d Paradis, M.; Vonsattel, J. P.; Gusella, J. F.; Beyreuther, K.; Masters, C. L.; Tanzi, R. E. *Science* **1994**, *265*, 1464−1467.

(15) (a) Todorich, B. M.; Connor, J. R. *Ann. N.Y. Acad. Sci.* **2004**, *1012*, 171−178. (b) Huang, X.; Moir, R. D.; Tanzi, R. E.; Bush, A. I.; Rogers, J. T. *Ann. N.Y. Acad. Sci.* **2004**, *1012*, 153−163. (c) Smith, D. G.; Cappai, R.; Barnham, K. J. *Biochim. Biophy. Acta* **2007**, *1768*, 1976−1990. (d) Hureau, C.; Faller, P. *Biochimie* **2009**, *91*, 1212−1217.

(16) Moreira, P. I.; Nunomura, A.; Zhu, X.; Lee, H.-G.; Aliev, G.; Smith, M. A.; Perry, G. In Veasey, S. C., Ed.; *Oxidative Neural Injury, Contemporary Clinical Neuroscience*; Humana: New York, 2009.

(17) (a) da Silva, G. F. Z.; Ming, L.-J. *Angew. Chem., Int. Ed.* **2005**, *44*, 5501−5504. (b) da Silva, G. F. Z.; Ming, L.-J. *Angew. Chem., Int. Ed.* **2007**, *46*, 3337−3341.

(18) Faria, A.; Pestana, D.; Teixeira, D.; Azevedo, J.; De Freitas, V.; Mateus, N.; Calhau, C. *Cell. Mol. Biol. Lett.* **2010**, *15*, 234−241.

(19) de Boer, V. C. J.; Dihal, A. A.; van der Woude, H.; Arts, I. C. W.; Wolffram, S.; Alink, G. M.; Rietjens, I. M. C. M.; Keijer, J.; Hollman, P. C. H. *J. Nutr.* **2005**, *135*, 1718−1725.

(20) (a) Ververidis, F.; Trantas, E.; Douglas, C.; Vollmer, G.; Kretzschmar, G.; Panopoulos, N. *Biotechnol. J.* **2007**, *2*, 1214−1234. (b) Ververidis, F.; Trantas, E.; Douglas, C.; Vollmer, G.; Kretzschmar, G.; Panopoulos, N. *Biotechnol. J.* **2007**, *2*, 1235−1249.

(21) (a) Havsteen, B. H. *Pharmacol. Ther.* **2002**, *96*, 67−202. (b) Dangles, O. *Curr. Org. Chem.* **2012**, *16*, 692−714.

(22) (a) Cao, G.; Sofic, E.; Prior, R. L. *Free Radicals Biol. Med.* **1997**, *22*, 749−760. (b) Kuo, S. M. *Crit. Rev. Oncol.* **1997**, *8*, 47−69. (c) Aziz, N. H.; Farag, S. E.; Mous,a, L. A. A.; Abo-Zaid, M. A. *Microbios* **1998**, *93*, 43−54. (d) Carlo, G. D.; Mascolo, N.; Izzo, A. A.; Capasso, F. *Life Sci.* **1999**, *65*, 337−353. (e) Erlund, I. *Nutr. Res. (N.Y.)* **2004**, *24*, 851−874. (f) Lule, S. U.; Xia, W. S. *Food Rev. Int.* **2005**, *21*, 367−388. (g) Mandel, S.; Amit, T.; Reznichenko, L.; Weinreb, O.; Youdim, M. B. H. *Mol. Nutr. Food Res.* **2006**, *50*, 229−234. (h) Kerboeuf, D.; Riou, M.; Guégnard, F. *Mini-Rev. Med. Chem.* **2008**, *8*, 116−128. (i) Yang, C. S.; Wang, X.; Lu, G.; Picinich, S. C. *Nat. Rev. Can.* **2009**, *9*, 429−439. (j) Velayutham, P.; Babu, A.; Liu, D. M. *Curr. Med. Chem.* **2008**, *15*, 1840−1850. (k) Butt, M. S.; Sultan, M. T. *Cri. Rev. Food Sci. Nutr.* **2009**, *49*, 463−473. (l) Yang, C. S.; Wang, H. *Mol. Nutr. Food Res.* **2011**, *55*, 819−831. (m) Ganesan, S.; Faris, A. N.; Comstock, A. T.; Wang, Q.; Nanua, S.; Hershenson, M. B.; Sajjan, U. S. *Antiviral Res.* **2012**, *94*, 258−271.

(23) Lambert, J. D.; Sang, S.; Yang, C. S. *Chem. Res. Toxicol.* **2007**, *20*, 583−585.

(24) Williams, R. J.; Spencer, J. P. E.; Rice-Evans, C. *Free Radicals Biol. Med.* **2004**, *36*, 838−849.

(25) (a) Da Silva, E. L.; Tsushida, T.; Terao, J. *Arch. Biochem. Biophys.* **1998**, *349*, 313−320. (b) Nagao, A.; Seki, M.; Kobayashi, H. *Biosci. Biotechnol. Biochem.* **1999**, *63*, 1787−1790.

(26) Furusawa, M.; Tanaka, T.; Ito, T.; Nishikawa, A.; Yamazaki, N.; Nakaya, K.-I.; Matsuura, N.; Tsuchiya, H.; Nagayama, M.; Iinuma, M. *J. Health Sci.* **2005**, *51*, 376−378.

(27) (a) Kaizer, J.; Balogh-Hergovich, É.; Czaun, M.; Csay, T.; Speier, G. *Coord. Chem. Rev.* **2006**, *250*, 2222−2233. (b) Grazul, M.; Budzisz, E. *Coord. Chem. Rev.* **2009**, *253*, 2588−2598.

(28) Lotito, S. B.; Fraga, C. G. *Free Radicals Biol. Med.* **1998**, *24*, 435−441.

(29) (a) Boadi, W. Y.; Iyere, P. A.; Adunyah, S. E. *J. Appl. Toxicol.* **2003**, *23*, 363−369. (b) Yokomizo, A.; Moriwaki, M. *Biosci. Biotechnol. Biochem.* **2005**, *69*, 693−699.

(30) Huang, Q.; Wu, L.-J.; Tashiro, S.-I.; Gao, H.-Y.; Onodera, S.; Ikejima, T. *J. Pharmacol. Sci.* **2005**, *98*, 16−24.

(31) Heo, H. J.; Lee, C. Y. *J. Agric. Food Chem.* **2005**, *53*, 1445−1448.

(32) Ossola, B.; Kääriäinen, T. M.; Männistö, P. T. *Expert. Opin. Drug Saf.* **2009**, *8*, 397−409.

(33) (a) Kampkoetter, A.; Timpel, C.; Zurawski, R. F.; Ruhl, S.; Chovolou, Y.; Proksch, P.; Waetjen, W. *Comp. Biochem. Physiol., Part B: Biochem. Mol. Biol.* **2008**, *149*, 314−323. (b) Pietsch, K.; Saul, N.; Menzel, R.; Stuerzenbaum, S. R.; Steinberg, C. E. W. *Biogerontology* **2009**, *10*, 565−578.

(34) Huebbe, P.; Wagner, A. E.; Boesch-Saadatmandi, C.; Sellmer, F.; Wolffram, S.; Rimbach, G. *Pharmacol. Res.* **2010**, *61*, 242−246.

(35) Haleagrahara, N.; Siew, C. J.; Mitra, N. K.; Kumari, M. *Neurosci. Lett.* **2011**, *500*, 139−143.

(36) Ansari, M. A.; Abdul, H. M.; Joshi, G.; Opii, W. O.; Butterfield, D. A. *J. Nutr. Biochem.* **2009**, *20*, 269−275.

(37) (a) Ono, K.; Yoshiike, Y.; Takashima, A.; Hasegawa, K.; Naiki, H.; Yamada, M. *J. Neurochem.* **2003**, *87*, 172−181. (b) Rivière, C.; Richard, T.; Quentin, L.; Krisa, S.; Mérillon, J.-M.; Monti, J.-P. *Bioorg. Med. Chem.* **2007**, *15*, 1160−1167. (c) Rivière, C.; Richard, T.; Vitrac, X.; Mérillon, J. M.; Valls, J.; Monti, J. P. *Bioorg. Med. Chem. Lett.* **2008**, *18*, 828−831. (d) Hirohata, M.; Hasegawa, K.; Tsutsumi-Yasuhara, S.; Ohhashi, Y.; Ookoshi, T.; Ono, K.; Yamada, M.; Naiki, H. *Biochemistry* **2007**, *46*, 1888−1899. (e) Kim, H.; Park, B.-S.; Lee, K.-G.; Choi, C. Y.; Jang, S. S.; Kim, Y.-H.; Lee, S.-E. *J. Agric. Food Chem.* **2005**, *53*, 8537−8541. (f) Akaishi, T.; Morimoto, T.; Shibao, M.; Watanabe, S.; Sakai-Kato, K.; Utsunomiya-Tate, N.; Abe, K. *Neurosci. Lett.* **2008**, *444*, 280−285. (g) Ushikubo, H.; Watanabe, S.; Tanimoto, Y.; Abe, K.; Hiza, A.; Ogawa, T.; Asakawa, T.; Kan, T.; Akaishi, T. *Neurosci. Lett.* **2012**, *513*, 51−56.

(38) He, X.; Park, H. M.; Hyung, S.-J.; DeToma, A. S.; Kim, C.; Ruotolo, B. T.; Lim, M. H. *Dalton Trans.* **2012**, *41*, 6558−6566.

(39) (a) Cherny, R. A.; Atwood, C. S.; Xilinas, M. E.; Gray, D. N.; Jones, W. D.; McLean, C. A.; Barnham, K. J.; Volitakis, I.; Fraser, F. W.; Kim, Y. S.; Huang, X. D.; Goldstein, L. E.; Moir, R. D.; Lim, J. T.; Beyreuther, K.; Zheng, H.; Tanzi, R. E.; Masters, C. L.; Bush, A. I. *Neuron* **2001**, *30*, 665−676. (b) Bush, A. I.; Tanzi, R. E. *Neurotherapeutics* **2008**, *5*, 421−432.

(40) (a) Cahoon, L. *Nat. Med.* **2009**, *15*, 356−359. (b) Mao, X.; Schimmer, A. D. *Toxicol. Lett.* **2008**, *182*, 1−6. (c) Benvenisti-Zarom, L.; Chen, J.; Regan, R. F. *Neuropharmacology* **2005**, *49*, 687−694. (d) Doraiswamy, P. M.; Finefrock, A. E. *Lancet Neurol.* **2004**, *3*, 431−434.

(41) Srivatsan, S. G.; Nigam, P.; Rao, M. S.; Verma, S. *Appl. Catal., A* **2001**, *209*, 327−334.

(42) (a) Espín, J. C.; Morales, M.; Varón, R.; Tudela, J.; García-Cánovas, F. *Anal. Biochem.* **1995**, *231*, 237−246. (b) Espín, J. C.; Morales, M.; García-Ruiz, P. A.; Tudela, J.; García-Cánovas, F. *J. Agric. Food Chem.* **1997**, *45*, 1084−1090.

(43) Rodríguez-López, J. N.; Escribano, J.; García-Cánovas, F. *Anal. Biochem.* **1994**, *216*, 205−212.

(44) Fenoll, L. G.; Garćia-Ruiz, P. A.; Varón, R.; García-Cánovas. *J. Agric. Food Chem.* **2003**, *51*, 7781−7787.

(45) (a) Polster, J.;Lachmann, H. *Spectrometric Titrations*; VCH: New York, 1989. (b) Huang, C. Y. *Methods Enzymol.* **1982**, *87*, 509−525.

(46) Wei, X.; Ming, L.-J. *Inorg. Chem.* **1998**, *37*, 2255−2262.

(47) Inubushi, T.; Becker, E. D. *J. Magn. Reson.* **1983**, *51*, 128−133.

(48) Tolman, W. B. *Acc. Chem. Res.* **1997**, *30*, 227−237.

(49) Segel, I. H. *Enzyme Kinetics: Behavior and Analysis of Rapid Equilibrium and Steady-State Enzyme Systems*; Wiley:New York, 1993; Chapters 3−4.

(50) (a) Kahn, V.; BenShalom, N.; Zakin, V. *J. Agric. Food Chem.* **1997**, *45*, 4460−4465. (b) Noh, J.-M.; Kwak, S.-Y.; Seo, H.-S.; Seo, J.-H.; Kim, B.-G.; Lee, Y.-S. *Bioorg. Med. Chem. Lett.* **2009**, *19*, 5586−5589.

(51) Demuro, A.; Mina, E.; Kayed, R.; Milton, S. C.; Parker, I.; Glabe, C. G. *J. Biol. Chem.* **2005**, *280*, 17294−17300.

(52) (a) Ming, L.-J. Biological Aspects of Metal Enolates. In *The Chemistry of Metal Enolates: The Patai's Series of the Chemistry of Functional Groups*; Zabicky, J., Ed.; Wiley: Chichester, 2009. (b) Ming, L.-J. Biological and Biomedical Aspects of Metal Phenolates. In *The Chemistry of Metal Phenolates: The Patai's Series of the Chemistry of Functional Groups*; Zabicky, J., Ed.; Wiley: Chichester, 2012.

(53) Zhao, B.; Guengerich, F. P.; Bellamine, A.; Lamb, D. C.; Izumikawa, M.; Lei, L.; Podust, L. M.; Sundaramoorthy, M.; Kalaitzis, J. A.; Reddy, L. M.; Kelly, S. L.; Moore, B. S.; Stec, D.; Voehler, M.; Falck, J. R.; Shimada, T.; Waterman, M. R. *J. Biol. Chem.* **2005**, *280*, 11599−607.

(54) Ming, L.-J.; Wei, X. *Inorg. Chem.* **1994**, *33*, 4617−4618.

(55) Zhou, J.; Wang, L. F.; Wang, J. Y.; Tang, N. *Trans. Met. Chem.* **2001**, *26*, 57−63.

(56) Bukhari, S. B.; Memon, S.; Tahir, M. M.; Bhanger, M. I. *J. Mol. Struct.* **2008**, *892*, 39−46.

(57) Jiménez-Aliaga, K.; Bermejo-Bescós, P.; Benedí, J.; Martín-Aragón, S. *Life Sci.* **2011**, *89*, 939−945.

(58) Erdogan, G.; Karadag, R. *Rev. Anal. Chem.* **2004**, *24*, 9−23.

(59) (a) Larsson, L.; Ohman, S. *Clin. Chem.* **1978**, *24*, 1962−1965. (b) Goldstein, D. A. Serum Calcium. In *Clinical Methods: The History, Physical, and Laboratory Examinations*, 3rd ed.; Walker, H. K., Hall, W. D., Hurst, J. W., Eds.; Butterworths: Boston, 1990; Chapter 143.

(60) (a) Bünzli, J.-C. G., Choppin, G. R., Eds.; *Lanthanide Probes in Life, Chemical and Earth Sciences*; Elsevier:Amsterdam, 1989. (b) Ming, L.-J. *Magn. Reson. Chem.* **1993**, *31*, S104−S109. (c) Ming, L.-J. In *Nuclear Magnetic Resonance of Paramagnetic Molecules*; La Mar, G. N., Ed.; NATO-ASI, Kluwer: Dordrecht, The Netherlands, 1995.

(61) Zhou, J.; Wang, L.-F.; Wang, J.-Y.; Tang, N. *J. Inorg. Biochem.* **2001**, *83*, 41−48.

(62) (a) Bertini, I.; Luchinat, C.; Parigi, G. *Solution NMR of Paramagnetic Molecules*; Elsevier: Amsterdam, 2001. (b) Ming, L.-J. Nuclear Magnetic Resonance of Paramagnetic Metal Centers in Proteins and Synthetic Complexes. In *Physical Methods in Bioinorganic Chemistry: Spectroscopy and Magnetism*; Que, L., Jr., Ed.; University Science Books:Sausalito, 2000.

(63) Bukharia, S. B.; Memon, S.; Mahroof-Tahir, M.; Bhanger, M. I. *Spectrochim. Acta, Part A* **2009**, *71*, 1901−1906.

(64) Grubel, K.; Rudzka, K.; Arif, A. M.; Klotz, K. L.; Halfen, J. A.; Berreau, L. M. *Inorg. Chem.* **2010**, *49*, 82−96.

(65) DeToma, A. S.; Choi, J.-S.; Braymer, J. J.; Lim, M. H. *ChemBioChem* **2011**, *12*, 1198−1201.

(66) (a) Kennedy, J. A.; Munro, M. H. G.; Powell, H. K. J.; Porter, L. J.; Foo, L. Y. *Aust. J. Chem.* **1984**, *37*, 885−892. (b) Jovanovic, S. V.; Steenken, S.; Tosic, M.; Marjanovic, B.; Simic, M. G. *J. Am. Chem. Soc.* **1994**, *116*, 4846−4851. (c) Herrero-Martinez, J. M.; Sanmartin, M.; Rosés, M.; Bosch, E.; Ràfols, C. *Electrophoresis* **2005**, *26*, 1886−1895.

(67) Ahmedova, A.; Paradowska, K.; Wawer, I. *J. Inorg. Biochem.* **2012**, *110*, 27−35.

(68) (a) Speier, G.; Fülöp, V.; Párkányi, L. *J. Chem. Soc., Chem. Commun.* **1990**, 512−513. (b) Balogh-Hergovich, E.; Speier, G.; Argay, G. *J . Chem. Soc., Chem. Commun.* **1991**, 551−552. (c) El Amrani, F. B. A.; Perelló, L.; Real, J. A.; González-Alvarez, M.; Alzuet, G.; Borrás, J.; García-Granda, S.; Montejo-Bernardo, J. *J. Inorg. Biochem.* **2006**, *100*, 1208−1218.

(69) (a) Baráth, G.; Kaizer, J.; Speier, G.; Párkányi, L.; Kuzmann, E.; Vértes, A. *Chem. Commun.* **2009**, 3630−3632. (b) Kaizer, J.; Baráth, G.; Pap, J.; Speier, G.; Giorgi, M.; Réglier, M. *Chem. Commun.* **2007**, 5235−5237. (c) Kaizer, J.; Pap, J.; Speier, G.; Párkányi, L. *Eur. J. Inorg. Chem.* **2004**, *2004*, 2253−2259. (d) Kaizer, J.; Pap, J.; Speier, G.; Réglier, M.; Giorgi, M. *Trans. Met. Chem.* **2004**, *29*, 630−633. (e) Lippai, I.; Speier, G.; Huttner, G.; Zsolnai, L. *Acta Crystallogr., Sect. C: Cryst. Struct. Commun.* **1997**, *53*, 1547−1549.

(70) Zhao, B.; Guengerich, F. P.; Bellamine, A.; Lamb, D. C.; Izumikawa, M.; Lei, L.; Podust, L. M.; Sundaramoorthy, M.; Kalaitzis, J A.; Reddy, L. M.; Kelly, S. L.; Moore, B. S.; Stec, D.; Voehler, M.; Falck, J. R.; Shimada, T.; Waterman, M. R. *J. Biol. Chem.* **2005**, *280*, 11599−11607.

(71) (a) de Souza, R. F. V.; De Giovani, W. F. *Redox Rep.* **2004**, *9*, 97−104. (b) Panhwar, Q. K.; Memon, S.; Bhanger, M. I. *J. Mol. Struct.* **2010**, *967*, 47−53. (c) Dimitrić Marković, J. M.; Marković, Z. S.; Brdarić, T. P.; Filipović, N. D. *Dalton Trans.* **2011**, *40*, 4560−4571.

(72) Kubo, I.; Kinst-Hori, I. *J. Agric. Food Chem.* **1999**, *47*, 4121−4125.

(73) Torreggiani, A.; Tamba, M.; Trinchero, A.; Bonora, S. *J. Mol. Struct.* **2005**, *744*, 759−766.

(74) Steiner, R. A.; Kalk, K. H.; Dijkstra, B. W. *Proc. Natl. Acad. Sci. U.S.A.* **2002**, *99*, 16625−16630.

(75) Lekka, Ch. E.; Ren, J.; Meng, S.; Kaxiras, E. *J. Phys. Chem. B* **2009**, *113*, 6478−6483.

(76) Du, H.; Guo, L.; Yan, S. S. *Antioxid. Redox Signaling* **2012**, *16*, 1467−1475.

(77) (a) Chen, Q.-S.; Kagan, B. L.; Hirakura, Y.; Xie, C.-W. *J. Neurosci. Res.* **2000**, *60*, 65−72. (b) Yu, J.-T.; Chang, R. C.-C.; Tan, L. *Prog. Neurobiol.* **2009**, *89*, 240−255.

(78) (a) Pollard, H. B.; Arispe, N.; Rojas, E. *Cell. Mol. Neurobiol.* **1995**, *15*, 513−526. (b) Arispe, N.; Rojas, E.; Pollard, H. B. *Proc. Natl. Acad. Sci. U.S.A.* **1993**, *90*, 567−571.
(79) Good, T. A.; Smith, D. O.; Murphy, R. M. *Biophys. J.* **1996**, *70*, 296−304.
(80) Mark, R. J.; Hensley, K.; Butterfield, D. A.; Mattson, M. P. *J. Neurosci.* **1995**, *15*, 6239−6249.
(81) (a) Cullen, W. K.; Suh, Y.-H.; Anwyl, R.; Rowan, M. J. *NeuroReport* **1997**, *8*, 3213−3217. (b) Ueda, K.; Shinohara, S.; Yagami, T.; Asakura, K.; Kawasaki, K. *J. Neurochem.* **1997**, *68*, 265−271. (c) He, L. M.; Chen, L. Y.; Lou, X. L.; Qu, A. L.; Zhou, Z.; Xu, T. *Brain Res.* **2002**, *939*, 65−75.
(82) Canzoniero, L. M. T.; Snider, B. J. *J. Alzheimer's Dis.* **2005**, *8*, 147−154.
(83) Lu, J.; Zheng, Y.-l.; Luo, L.; Wu, D.-m.; Sun, D.-x.; Feng, Y.-j. *Behav. Brain Res.* **2006**, *171*, 251−260.
(84) Shimmyo, Y.; Kihara, T.; Akaike, A.; Niidome, T.; Sugimoto, H. *J. Neurosci. Res.* **2008**, *86*, 1836−1845.
(85) Sakanashi, Y.; Oyama, K.; Matsui, H.; Oyama, T. B.; Oyama, T. M.; Nishimura, Y.; Sakai, H.; Oyama, Y. *Life Sci.* **2008**, *83*, 164−169.
(86) Weng, Z.; Zhang, B.; Asadi, S.; Sismanopoulos, N.; Butcher, A.; Fu, X.; Katsarou-Katsari, A.; Antoniou, C.; Theoharides, T. C. *PLoS ONE* **2012**, *7*, e33805.
(87) Djelili, H.; Arrar, L.; Naline, E.; Devillier, P. *China's Med.* **2012**, *3*, 94−100.
(88) Beking, K.; Vieira, A. *Public Health Nutr.* **2010**, *13*, 1403−1409.
(89) Drake, J.; Link, C. D.; Butterfield, D. A. *Neurobiol. Aging* **2003**, *24*, 415−420.
(90) (a) Pappolla, M. A.; Chyan, Y. J.; Omar, R. A.; Hsiao, K.; Perry, G.; Smith, M. A.; Bozner, P. *Am. J. Pathol.* **1998**, *152*, 871−877. (b) Smith, M. A.; Hirai, K.; Hsiao, K.; Pappolla, M. A.; Harris, P. L.; Siedlak, S. L.; Tabaton, M.; Perry, G. *J. Neurochem.* **1998**, *70*, 2212−2215. (c) Pratico, D.; Uryu, K.; Leight, S.; Trojanoswki, J. Q.; Lee, V. M. *J. Neurosci.* **2001**, *21*, 4183−4187.
(91) (a) Castellani, R. J.; Lee, H.-G.; Zhu, X.; Nunomura, A.; Perry, G.; Smith, M. A. *Acta Neuropathol.* **2006**, *111*, 503−509.